Available online at www.sciencedirect.com
ScienceDirect
Journal of the European Ceramic Society 30 (2010) 1453–1460
www.elsevier.com/locate/jeurceramsoc

Crystallization behavior, microstructure and dielectric properties of lead titanate glass ceramics in the presence of Bi_2O_3 as a nucleating agent

S. Golezardi, V.K. Marghussian *, A. Beitollahi, S.M. Mirkazemi

Department of Materials, Iran University of Science and Technology, Narmak, Tehran 16844, Iran

Received 8 August 2009; received in revised form 29 October 2009; accepted 26 November 2009
Available online 23 December 2009

Abstract

The crystallization behavior of $PbO–TiO_2–B_2O_3–SiO_2$ glasses in the presence of Bi_2O_3 as a nucleating agent were studied utilizing XRD, DTA, SEM. The glass samples heat treated in the range of 557–630 °C for different soaking times, all developed $PbTiO_3$ (PT) with perovskite structure. It was found that the addition of 0.5–1.0 mol% Bi_2O_3 resulted in the formation of homogenous, nano-structured glass ceramics with a mean crystallite size of 20–25 nm and $PbTiO_3$ as the major crystalline phase. The dielectric constant and dissipation factors for the prepared glass ceramics were in ~140–400 and ~0.04–0.4 ranges respectively.

Keywords: Glass ceramics; Titanates; Perovskites; Dielectric properties; Nanocomposites

1. Introduction

Because of their outstanding ferroelectric, piezoelectric and pyroelectric properties, the great potential of $BaTiO_3$ and $PbTiO_3$ ceramics for certain applications have been recognized for many decades. It is, however, difficult to prepare these materials via conventional ceramic route, because of their poor sinterability and fragility. There have been many attempts to utilize other fabrication methods such as glass ceramic process to make dense ceramics, with more controlled microstructure and better properties in this system. Despite the extensive research carried out to investigate and develop fine grained, pore-free glass ceramics containing $BaTiO_3$, $PbTiO_3$ and $NaNbO_3$ ferroelectric phases, for decades[1–14] they are still under investigation.[15–19]

The controlled crystallization of the perovskite-type lead titanate ($PbTiO_3$) was first reported by Herczog.[1] The crystallization process of $PbTiO_3$ in glasses was also studied by Bergeron and Russell[2] who reported that nucleation proceeded via glass-in-glass phase separation. Kokubo and Tashiro[3,4] have studied glass formation and the subsequent controlled crystallization of $SiO_2–Al_2O_3–TiO_2–PbO$ glasses. Their prepared glass specimens were crystallized in a subsequent heat treatment in the temperature range 620–750 °C. In this process it was either possible to precipitate perovskite type $PbTiO_3$ from the initial pyrochlore-type $PbTi_3O_7$ phase or from the cubicoid $PbTiO_3$ crystals. Several studies on to the crystallization of glass ceramics containing ferroelectric $PbTiO_3$ phase have demonstrated the close relationship existing between the microstructure and dielectric properties of these glass ceramics.[5,6,9–11,14,16] Thakur et al.[15,20] reported that the small additions of Bi_2O_3 nucleating agent markedly affected crystallization behavior and resulting microstructure of strontium titanate borosilicate glass ceramics containing alkali oxides.

In the present work, an attempt was made to study the effect of addition of Bi_2O_3 as a nucleating agent on the crystallization behavior, microstructure and dielectric properties of $PbTiO_3$ (PT) glass ceramics. To the authors knowledge this nucleating agent has never been used before in lead titanate glass ceramics.

2. Experimental procedure

In order to prepare stable glasses, by giving consideration to the compositions used by other investigators in the same field and on the basis of preliminary experimental results obtained by the present investigators it was first decided to prepare glass compositions containing at least 30 mol% glass forming oxides

* Corresponding author. Tel.: +98 21 73912814; fax: +98 21 77240480.
E-mail address: v_k_marghus@yahoo.com (V.K. Marghussian).

0955-2219/$ – see front matter © 2009 Elsevier Ltd. All rights reserved.
doi:10.1016/j.jeurceramsoc.2009.11.016

($SiO_2 + B_2O_3$). In this way an initial glass composition was formulated by assuming a stoichiometric ratio of $PbO/TiO_2 = 1$ as 35 PbO–35 TiO_2–20 SiO_2–10 B_2O_3. This glass specimen was crystallized during cooling. Subsequently by increasing the PbO/TiO_2 ratio in 0.25 steps, it became possible to prepare a stable glass with the ratio of $PbO/TiO_2 = 2$ showing no signs of crystallization (as proved by XRD). The above glass, entitled as base glass in the following discussion, had a nominal composition of 46.67 PbO–23.33 TiO_2–20 B_2O_3–10 SiO_2 (mol%). Other specimens were prepared with the addition of 0.5 and 1.0 mol% Bi_2O_3 to the base composition (specimens S0.5 and S1 respectively). Batches weighting 50 g containing the proportionate amounts of reagent grade chemicals Pb_3O_4, TiO_2, H_3BO_3, SiO_2 and Bi_2O_3 were thoroughly mixed in an agate mortar and melted in alumina crucibles in the temperature range of 1450–1470 °C. The melts were kept for 20 min at their respective melting temperatures and were stirred thoroughly to ensure better homogenization before casting into stainless steel molds. The glasses were then annealed at 400 °C for 2 h and their amorphous nature checked by X-ray diffraction. In order to determine the glass transition and crystallization temperatures, the glass specimens were subjected to differential thermal analysis (DTA) utilizing a STA1400 Polymer Laboratories thermal analyzer using Al_2O_3 powder as a reference material. The heating rate was 10 °C min^{-1} and the experiments were carried out in ambient −1200 °C range. On the basis of the DTA results, glasses were crystallized by subjecting them to various heat-treatment schedules. X-ray diffraction patterns for resulting glass ceramic samples were recorded employing JEOL-JDX-8030 diffractometer using nickel filtered Cu Kα radiation. Working voltage and current were 40 kV and 80 mA, respectively. The patterns were recorded in the 2θ range of 5–80°, in a step-scanning mode with a step size of 0.04° and a 0.75 s constant time per step. The crystalline phases in each glass ceramic sample were identified by comparing their XRD patterns with the standard patterns of various crystalline phases anticipated to be formed in the specimens under the given processing conditions. The glass ceramic samples were polished, etched with a solution containing equal volumes of 5% HNO_3 and 5% HF for 50 s and then coated with a thin film of gold for scanning electron microscopy (SEM) observations (PHILIPS-XL30). For measurements of dielectric properties of glass ceramics, both surfaces of samples were ground and polished using SiC powder for attaining smooth surfaces to a thickness of 1 mm. The electrodes were made by applying silver paint on both sides of the specimens and drying at room temperature for 24 h. Capacitance and dissipation factors of the samples were measured at 100 kHz at room temperature utilizing LCR-800 SERIES (GW InsTek®) LCR meter.

3. Results and discussion

3.1. Differential thermal analysis (DTA) results

DTA traces of various glass samples are presented in Fig. 1. For all the specimens a deviation in the base line is observed in the temperature range of 440–475 °C (endothermic effect). This is attributed to the change in specific heat occurring in glass transition range. The onset temperature of the dip is usually attributed to the glass transition temperature (T_g) whereas the minimum is assigned to the dilatometeric softening point (T_s). The exothermic peaks (T_c) are usually related to the glass crystallization. The results have summarized in Table 1.

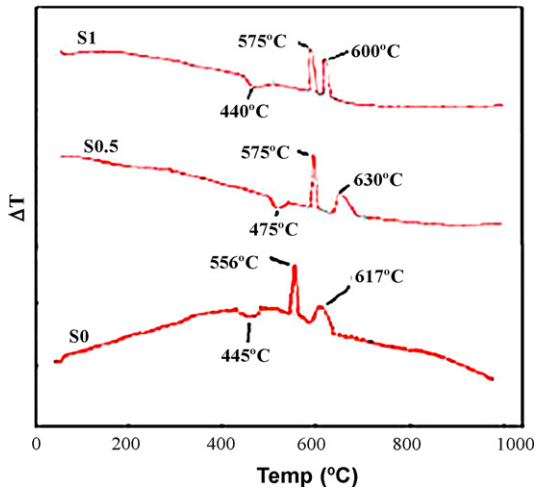

Fig. 1. DTA traces of glass specimens.

It can be seen that for all glass samples, two exothermic crystallization peaks T_{c_1} and T_{c_2} appear in DTA plots.

3.2. X-ray diffraction and crystallization results

On the basis of DTA results, glass samples were subjected to various heat-treatment procedures. Fig. 2 depicts the XRD patterns of specimen S0 (lacking Bi_2O_3) after 1 h heat treatment at its first (S01) and second (S02) DTA exo-peak temperatures. It can be seen that cubic and tetragonal $PbTiO_3$ were developed as the major crystalline phases at the first and second peaks respectively.

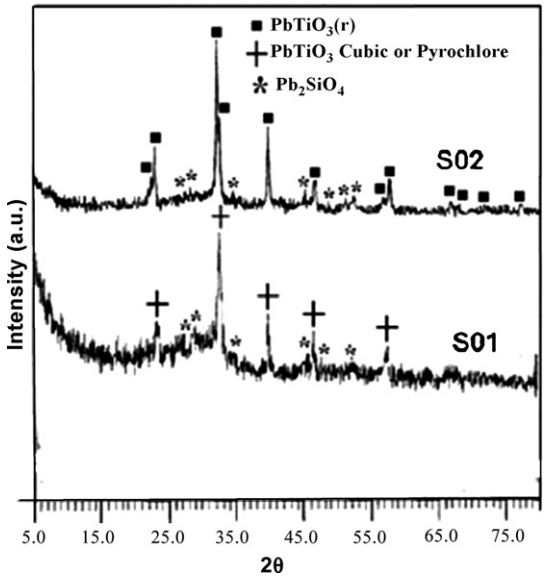

Fig. 2. XRD patterns of base glass after crystallization at its first (S01) and second (S02) DTA peaks.

Table 1
Characteristic DTA peak temperatures of glass samples.

Sample	T_g (°C) glass transition temp.	T_s (°C) dilatometeric softening point	T_{c_1} (°C) first cryst. temp.	T_{c_2} (°C) second cryst. temp.
S0 (base glass)	445	470	556	617
S0.5	475	490	575	630
S1	440	463	575	600

XRD patterns of the heat-treated glasses S0.5 containing 0.5% Bi_2O_3 are presented in Fig. 3a. These samples were heat treated at their respective first (S0.5-1) and second (S0.5-2) DTA peak temperatures for 1 h.

Fig. 3b depicts XRD patterns of the heat-treated glasses containing 1% Bi_2O_3, heat treated at their respective first (S1-1) and second (S1-2) DTA exo-peak temperatures for 1 h.

It can be seen that all four glass ceramic samples represented in Fig. 3a and b contained tetragonal perovskite as the major phase and Pb_2SiO_4 as the minor phase. The shift in XRD peak positions in specimens of composition S1 in comparison with other glass ceramic samples is possibly due to the entering of Bi^{3+} ions into the $PbTiO_3$ crystal structure and formation of solid solutions in these samples.

To study the effect of holding time at nucleation temperature (T_N) on phase development and microstructure of the glass samples they were subjected to various "nucleating" heat treatments. The nucleation temperature (T_N) of a glass is generally located between T_g and T_s and in this work it was taken as

$$T_N = \frac{T_g + T_S}{2}.$$

XRD patterns of some glass ceramic samples prepared from glasses S0, S0.5 and S1 after nucleation and crystallization are presented in Fig. 4a and b.

Samples S0-N1 and S0-N3 that prior to crystallization were subjected to a nucleation process for 1 and 3 h, respectively were found to contain tetragonal perovskite lead titanate as the major phase with a trace amount of Pb_2SiO_4. The glass ceramic samples S0.5-N1 and S0.5-N3 were again found to contain tetragonal perovskite as the major phase and Pb_2SiO_4 as the minor phase, but it is clear that the intensity of XRD peaks are increased in S0.5 series, due to the addition of 0.5 mol% Bi_2O_3 to the system (Fig. 4a and b). Samples S1-N1 and S1-N3 contained a solid solution of perovskite lead titanate as the major phase with a trace amount of Pb_2SiO_4. In XRD patterns of the latter glass ceramic samples it seems that the peaks corresponding to (1 0 1) ($I/I_0 = 100$) and (1 1 0), have merged. This is possibly due to the entrance of Bi^{3+} ions into the $PbTiO_3$ crystal structure and formation of solid solutions in these samples.

Table 2 summarizes the heat-treatment conditions and crystallization products for all glass ceramic specimens.

The lattice parameters '*c*' and '*a*' and *c*/*a* ratio of tetragonal lead titanate phase developed in glass ceramic samples were also

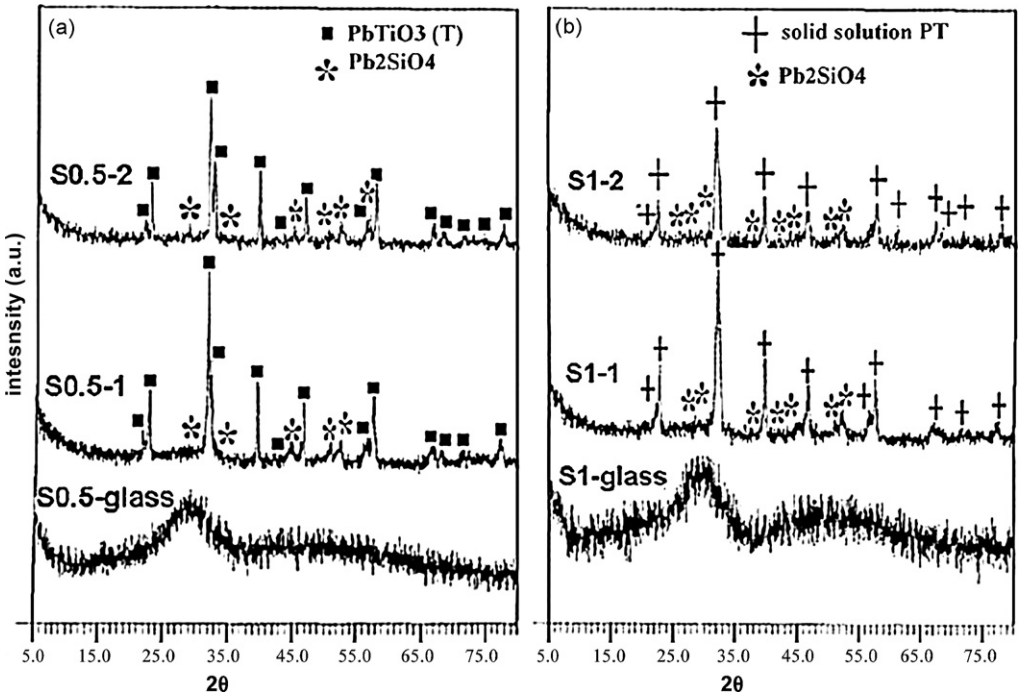

Fig. 3. (a) XRD patterns of specimen (S0.5) containing 0.5% Bi_2O_3 after crystallization at its first (S0.5-1) and second (S0.5-2) DTA peaks. (b) XRD patterns of specimen (S1) containing 1% Bi_2O_3 after crystallization at its first (S-1) and second (S-2) DTA peaks.

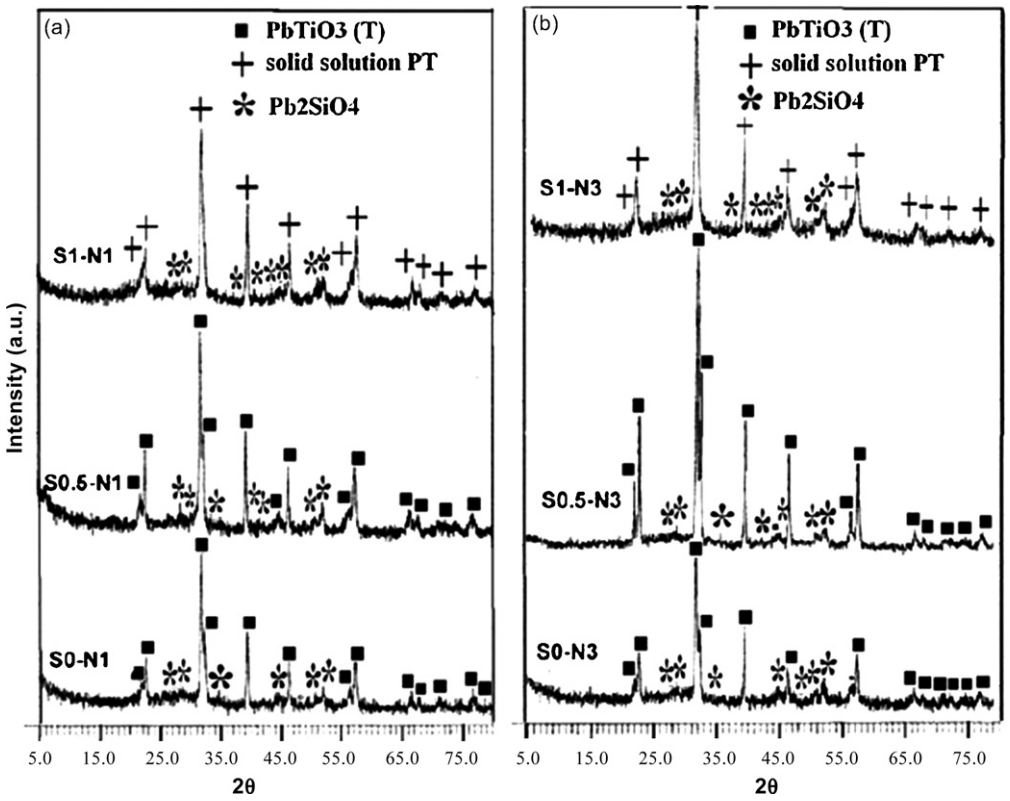

Fig. 4. (a) XRD patterns of specimens lacking Bi_2O_3 (S0-N1) and containing 0.5% and 1% Bi_2O_3 (S0.5-N1 and S1-N1 respectively) after 1 h nucleation at TN and crystallization at their first DTA peak for 1 h. (b) XRD patterns of specimens lacking Bi_2O_3 (S0-N3) and containing 0.5% and 1% Bi_2O_3 (S0.5-N3 and S1-N3 respectively) after 3 h nucleation at TN and crystallization at their first DTA peak for 1 h.

Table 2
Heat-treatment conditions and crystalline phases developed in various glass ceramic samples.

Specimen code	Nucleation temp. T_N (°C)	Holding time at T_N (h)	Crystallization temp. T_c (°C)	Holding time at T_c (h)	Crystalline phases
S0-1	460	0	560	1	PT(c)
S0-2	460	0	620	1	PT(t) + PS
S0-N1	460	1	620	1	PT(t) + PS
S0-N3	460	3	620	1	PT(t) + PS
S0.5-1	485	0	575	1	PT(t) + PS
S0.5-2	485	0	630	1	PT(t) + PS
S.0.5-N1	485	1	575	1	PT(t) + PS
S0.5-N3	485	3	575	1	PT(t) + PS
S1-1	455	0	575	1	PT(ss) + PS
S1-2	455	0	600	1	PT(ss) + PS
S1-N1	455	1	575	1	PT(ss) + PS
S1-N3	455	3	575	1	PT(ss) + PS

S0 = base glass, S0.5 = base glass + 0.5 mol% Bi_2O_3, S1 = base glass + 1 mol% Bi_2O_3, PT = $PbTiO_3$, t = tetragonal, c = cubic, ss = solid solution, PS = Pb_2SiO_4.

calculated using Eq. (1) below.

$$\sin^2_{h\,k\,l}\theta = \frac{\lambda^2}{4a^2}(h^2 + k^2) + \frac{\lambda}{4c^2}l^2 \quad (1)$$

where θ is diffraction angle corresponding to *hkl* planes in degree, λ the wave length of the X-ray used in the experiment, '*a*' and '*c*' are lattice parameters. The shift in XRD peak positions of $PbTiO_3$ in glass ceramic samples as compared with the standard $PbTiO_3$ is reflected in the values of their lattice parameters (Table 3). It may due to the formation of lead titanate perovskite solid solution crystallites.[6]

It can be seen that the lattice parameters '*a*' of the perovskite phases developed in the glass ceramic samples S0-N3 and S0.5-N3 are less than the reported value of standard $PbTiO_3$, whereas the same parameter is higher than standard for the specimen S1-N3 It is also obvious that the lattice parameters '*c*' are less than the standard for all of the three specimens and decrease in the order of S0.5-N3 > S1-N3 > S0-N3, hence it is closer to the standard value for the specimen S0.5-N3. In this way the *c/a* ratios of the perovskite titanate phases developed in all of the above specimens are less than the standard value but this ratio is closer to the standard for specimen S0.5-N3 and the smallest value corresponds to specimen S1-N3 containing 1 mol% Bi_2O_3. This

Table 3
Crystal structure, lattice parameters and axial ratios of perovskite lead titanate phase developed in some glass ceramic samples.

Sample	Crystal structure	a (Å)	c (Å)	c/a
Standard $PbTiO_3$	Tetragonal	3.899	4.1532	1.065
S0-N3	Tetragonal	3.880	3.999	1.031
S0.5-N3	Tetragonal	3.880	4.076	1.050
S1-N3	Tetragonal	3.915	4.003	1.022

marked reduction of the *c/a* ratio and its approach to the value of ~1 (cubic phase) leading to more symmetrical crystals is probably the cause of the merging of XRD peaks corresponding to (1 0 1) and (1 1 0) planes, as mentioned above.

In perovskite titanate phase, the increase of *c/a* ratio is desirable, because the higher *c/a* ratio normally increases the polarizability and improves the ferroelectric properties.[21]

3.3. Microstructural studies

Although some of the as received glasses; especially the specimens containing the nucleating agent, showed very faint signs of phase separation at high magnification SEM observations, but the glass-in-glass phase separation only became quite visible after a hold at the nucleation temperature. Fig. 5 shows the scanning electron micrograph of glass sample S0.5 after heat treatment at the nucleation temperature of 485 °C for1 h. The micrograph exhibits a glass-in-glass phase separation, apparently occurred by a spinodal decomposition mechanism.

Figs. 6–9 depict the SEM micrographs of glass ceramic samples obtained by heat treating some glasses according to the procedure represented in Table 2. Microstructure of the glass ceramic sample S0-N1 (Fig. 6) shows the crystallites of perovskite titanate phase distributed in the glassy matrix. In addition to equiaxed crystallites, a few elongated crystallites are also observable, which are the result of exaggerated grain growth. Fig. 7 shows scanning electron micrograph of glass-ceramic sample S0.5-N1. It seems that upon the addition of the nucleating agent, even in the small quantity of 0.5 mol%, the size of crystallites became much finer, interconnected and uniform, in comparison with the specimen S0-N1 lacking the Bi_2O_3 nucleant. The microstructures of specimen S1-N1 and S1-N3 (Figs. 8 and 9) show the continuation of the trend of particle size reduction upon increasing the content of the nucleating agent and the nucleation time.

It is interesting to note that the actual crystallite sizes of the specimens as calculated from Scherrer's equation are much smaller than the particles observed in the SEM micrographs. These sizes were ~40, 25 and 20 nm for specimens S0-N3, S0.5-N3 and S1-N3, respectively. In fact most of the particles

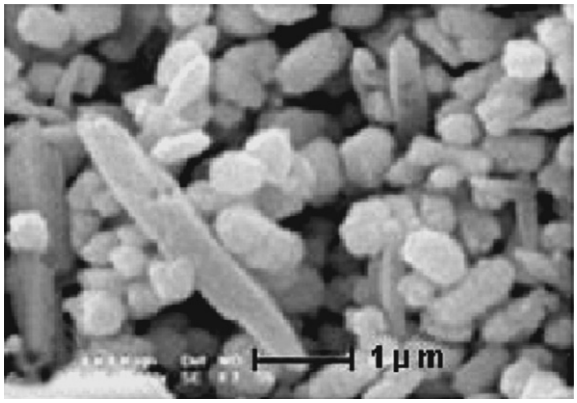

Fig. 6. SEM micrograph of specimen S0 (with no nucleant) after nucleation at 460 °C for 1 h and crystallization at 620 °C for 1 h.

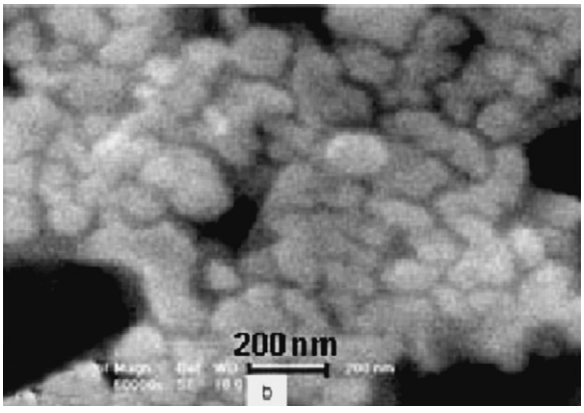

Fig. 7. SEM micrograph of specimen S0.5 with 0.5% Bi_2O_3, after nucleation at 485 °C for 1 h and crystallization at 575 °C for 1 h.

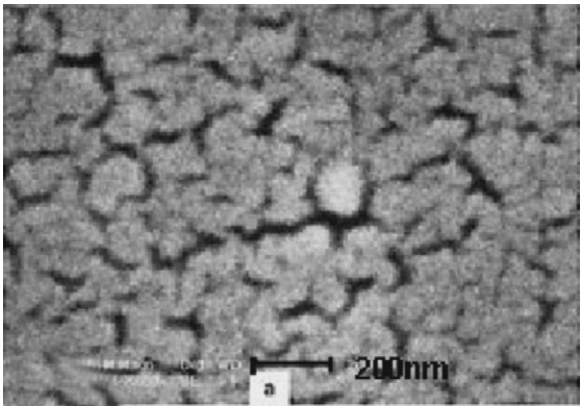

Fig. 5. SEM micrograph showing phase separation in glass S0.5 after nucleation at 485 °C for 1 h.

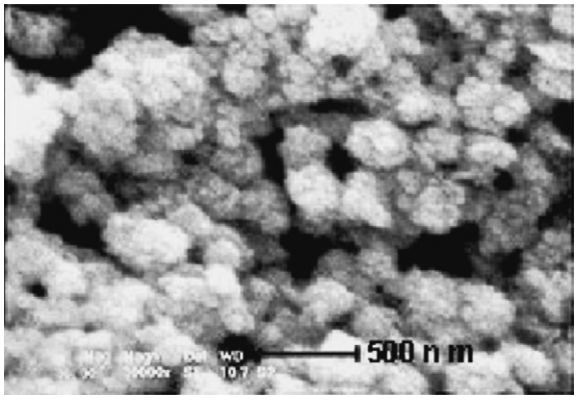

Fig. 8. SEM micrograph of specimen S1 with 1% Bi_2O_3, after nucleation at 455 °C for 1 h and crystallization at 575 °C for 1 h.

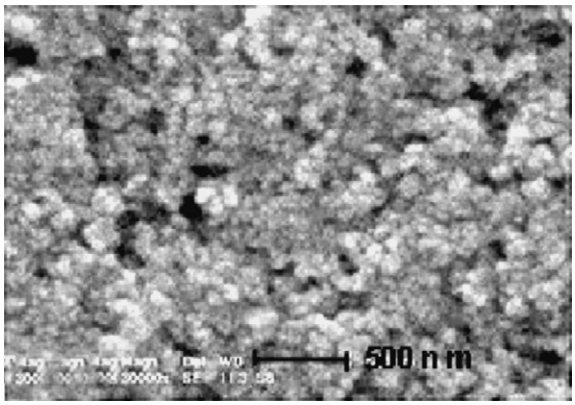

Fig. 9. SEM micrograph of specimen S1 with 1% Bi_2O_3 after nucleation at 455 °C for 3 h and crystallization at 575 °C for 1 h.

observed in the microstructures are crystalline aggregates comprising of numerous fine crystallites. Some micrographs (e.g. Fig. 8) clearly show the aggregates of tiny crystallites.

Therefore it can be concluded that Bi_2O_3 has actually acted as an effective nucleation agent in these glasses and by increasing the nucleation rate led to finer microstructures.

It can be postulated that like most of the nucleants in glass systems, Bi_2O_3 probably initiated or intensified the phase separation process in these glasses. The comparison of the glass microstructures, as stated above, clearly showed much more enhanced phase separation in the glass specimens containing Bi_2O_3. Other investigators also reported the occurrence of phase separation in the glasses of similar composition in the presence of the latter oxide.[12,15]

In the lead borosilicate glass investigated here, a stable glass network would be consisted of SiO_4, BO_3 and BO_4 network forming unites linked through the oxygens. Therefore B–O–B, Si–O–Si and B–O–Si bonds would be present in the glass network. With the addition of modifier ions, these linkages would be broken giving rise to non-bridging oxygens. On the other hand in glasses with high PbO content, the coordination number of Pb is four suggesting that PbO acts as a network former consisting of PbO_4 tetrahedra.[22] These tetrahedra are connected to the other structural unites. Therefore it seems that TiO_2 which is preferentially present in the glass structure, as TiO_6 octahedra is the only oxide that would assume the glass modifier role in this glass (though as an intermediate oxide it could also act as a network former in some conditions). When the concentration of TiO_2 is high and the desired coordination number of Ti^{+4} cations are not satisfied, they could become structurally ordered with respect to each other. These structurally ordered regions produce microheterogenities in the glass structure which may lead to glass-in-glass phase separation. On the other hand, if the added Bi^{+3} ions to the glass structure act as glass formers (like Pb^{+2}), the drive to satisfy the oxygen coordination along with their relatively high ionic field strength, in comparison with Pb^{+2}, adds an additional instability factor to the previously existing problem of TiO_2. This leads to the initiation of phase separation in these glasses. The phase separation would result in the formation of regions of high TiO_2 content in the glass, which become effective nucleation centres and accelerate the nucleation step of $PbTiO_3$ crystallization, hence affecting the microstructure and properties of resulting glass ceramics. This idea of $PbTiO_3$ crystallization within the phase separated regions of high TiO_2 content have also been proposed by other investigators.[23]

Table 4
Dielectric constant (ε_r) and dissipation factor (D) at room temperature and frequencies of 100 kHz for the prepared glass ceramic samples.

Sample	ε_r	D
S0 glass	90.2	0.031
S0-N1	256.1	0.24
S0-N3	273	0.21
S0.5-N1	274	0.33
S0.5-N3	392.2	0.39
S1-N1	173.9	0.041
S1-N3	139.8	0.044

3.4. Dielectric properties

Dielectric constant (ε_r) and dissipation factor (D) at room temperature are shown in Table 4. Obviously the dielectric constant increases and decreases with addition of 0.5 and 1 mol% Bi_2O_3 to the base glass composition, respectively. It is interesting to note that increasing the holding time at nucleation temperature led to a marked increase of dielectric constant (ε_r) in the glass ceramic with 0.5 mol% Bi_2O_3. It may be caused by increasing the percentage of crystallinity in this specimens, as shown in XRD traces.

The measured dielectric constant for the above specimen is amongst the highest values reported so far for these type of glass ceramics.

Several factors such as grain size, its distribution and morphology, secondary phases, crystal clamping and interconnectivity of crystallites in the glassy matrix affect the value of dielectric constant; hence, it is quite difficult to explain the exact causes behind the experimental observations in this regard. However, an attempt is made here to relate the dielectric properties to microstructural and structural observations.

The microstructure of glass ceramic sample S0.5-N1 as shown in Fig. 7 exhibited fine crystallites of isolated perovskite lead titanate uniformly distributed in the glassy matrix.

A glass ceramic material is usually comprised of one or several crystalline phases distributed in a glassy matrix. Therefore it can be expected that the dielectric properties of the material are influenced by the content, composition, particle sizes and the way of distribution of its constituent phases. The crystalline phases, glass matrix and the interfacial region existing between them each may have its own contribution to the polarization processes occurring in the glass ceramic material as a whole.

The resistivity differences existing between crystals and glassy matrix may cause a charge build-up occurring in the interfacial region. This usually leads to a large space charge polarization and elevation of dielectric constant values.[15,24,25] Therefore it can be deduced that the reduction of crystallite sizes of the lead titanate phase, due to the addition of Bi_2O_3 nucleant, such as in specimens S0.5-N1 and S0.5-N3, by extending the

interfacial region has resulted in higher polarization effects and larger dielectric constant values.

On the other hand in the glass ceramic S1-N3, containing 1 mol% Bi_2O_3, the drop of (ε_r) value in the specimen can possibly be attributed to the contribution of the crystalline phase. It seems that in the above specimen despite the observed smallest size of perovskite crystallites, the dissolution of Bi^{+3} ions in $PbTiO_3$ that reduced the *c*/*a* ratio in the crystal lattice, played the dominant role and decreased the dielectric constant value. This can be related to the reduction of polarization effects due the smaller value of the *c*/*a* ratio in the latter specimen as discussed above. On the other hand it can also postulated that the entrance of Bi^{+3} ions as donors into the crystal structure of the perovskite phase, replacing Pb^{+2}, perhaps has resulted in the lowering of resistivity of the latter phase by creating point defects that resulted in n-type semiconducting effects. A similar effect has previously been reported for La^{+3} additions to barium titanate dielectric materials.[26] On the basis of the values of resistivities reported by other investigators[15] and considering the relatively low value of dissipation factor determined for the glass specimen in the present study (Table 4) it can be assumed that crystalline phases had higher resistivity values as compared to the glassy phase in the studied specimens. In this condition it can be assumed that the semiconducting effect mentioned above might have reduced the resistivity difference existed between crystalline and glassy phases in glass ceramics and resulted in less charge build-up at the interfacial regions that led to lower space charge polarization values. The latter effect might have played a predominant role in reducing the dielectric constant upon addition of Bi_2O_3 to the base composition in amounts exceeding 0.5 mol%.

It can also be inferred that increasing the nucleation time from 1 to 3 h in the case of specimen S0 (lacking nucleation agent) had almost no effect upon the values of its dielectric constant and dissipation factor (Table 4). This is an indication of the ineffectiveness of prolonged nucleation for the above specimen, whereas in the case of specimen S0.5 the prolonged nucleation have exerted a marked effect as discussed above.

It is also interesting to note that in the case of specimen S1 the dissipation (loss) factor shows an almost 10-fold drop as compared to the specimen S0.5. It is again very difficult to give a precise explanation to this, but perhaps it can mainly be attributed to the space charge polarization effect. The relatively high dissipation factor in specimen S0.5-N3, like its large dielectric constant value, can be attributed to large space charge polarization effect as discussed above. In this way the marked drop in dissipation factors in specimens of series S1 in comparison with their S0.5 counterparts can be attributed to the reduced resistivity difference and less pronounced space charge polarization in specimens S1 owing to the semiconducting effect of added Bi^{+3} ions as discussed above.

4. Conclusions

The crystallization behavior and microstructural characteristics of various glass ceramic samples in the 46.67 PbO–23.33 TiO_2–20 B_2O_3–10 SiO_2 mol% system with addition of 0.5 and 1.0 mol% Bi_2O_3 as a nucleating agent have been studied. Perovskite titanate was the major phase in all the glass ceramic samples. The formation of nano-structured $PbTiO_3$ glass ceramics was confirmed for specimen containing 0.5 mol% Bi_2O_3 by SEM and XRD results. In glass ceramic containing Bi_2O_3, the degree of phase separation is higher and the nucleation proceeds faster during heat treatment. This resulted in fine-grained microstructures. The magnitude of the permittivity (ε_r) for the specimens containing 0.5 mol% Bi_2O_3, heat treated for 3 h at 485 °C and 1 h at 575 °C was ∼390 that was the highest value amongst all the heat-treated samples. This value is also high in comparison with most of the reported values for these glass ceramics.

References

[1]. Herczog A. Microcrystalline $BaTiO_3$ by crystallization from glass. *J Am Ceram Soc* 1964;**47**:107–15.

[2]. Bergeron CG, Rusell CK. Nucleation and growth of lead titanate from a glass. *J Am Ceram Soc* 1965;**48**:115–8.

[3]. Kokubo T, Tashiro M. Thin-film capacitors made from glass-ceramic containing PbO and TiO_2. *J Ceram Soc Jpn* 1970;**78**:58–63.

[4]. Kokubo T, Tashiro M. Dielectric properties of fine-grained $PbTiO_3$ crystals precipitated in a glass. *J Non-Cryst Solids* 1974;**13**:328–40.

[5]. Grossman DG, Isard JO. Lead titanate glass–ceramics. *J Am Ceram Soc* 1969;**52**:230–1.

[6]. Grossman DG, Isard JO. Crystal clamping in $PbTiO_3$, glass–ceramics. *J Mater Sci* 1969;**4**:1059–63.

[7]. Borrelli NF, Layton MM. Dielectric and optical properties of transparent ferroelectric glass–ceramic systems. *J Non-Cryst Solids* 1971;**6**:197–212.

[8]. Herczog A. Barrier layers in semiconducting barium titanate glass–ceramics. *J Am Ceram Soc* 1984;**67**:484–90.

[9]. Lynch SM, Shelby JE. Crystal clamping in lead titanate glass–ceramics. *J Am Ceram Soc* 1984;**61**:424–7.

[10]. Saegusa K, Rhine WE, Bowen HK. Effect of composition and size of crystallite on crystal phase in lead barium titanate. *J Am Ceram Soc* 1993;**76**:1505–12.

[11]. Shyu JJ, Yang JS. Crystallization of PbO–BaO–TiO_2–Al_2O_3–SiO_2 glass. *J Am Ceram Soc* 1995;**78**:1463–8.

[12]. Thakur OP, Kumar D, Parkash O, Pandey L. Dielectric and microstructural behavior of strontium titanate borosilicate glass ceramic system. *Bull Mater Sci* 1995;**18**:557–85.

[13]. Lee SW, Shim KB, Auh KH, Knott P. Ferroelectric anomaly in the differential thermal analysis of $PbTiO_3$ glass. *Mater Lett* 1999;**38**:356–9.

[14]. Lee SW, Shim KB, Auh KH, Knott P. Activation energy of crystal growth in $PbTiO_3$ glass using differential thermal analysis. *J Non-Cryst Solids* 1999;**248**:127–36.

[15]. Thakur O, Kumar P, Parkash D, Pandey OL. Electrical characterization of strontium titanate borosilicate glass ceramics system with bismuth oxide addition using impedance spectroscopy. *Mater Chem Phys* 2003;**78**:751–9.

[16]. Ruiz-Valde's JJ, Gorokhovsky AV, Escalante-García JI, Mendoza-Sua'rez G. Glass–ceramic materials with regulated dielectric properties based on the system BaO–PbO–TiO_2–B_2O_3–Al_2O_3. *J Eur Ceram Soc* 2004;**24**:1505–8.

[17]. Sahu AK, Kumar D, Parkash O, Thakur OP, Prakash C. Effect of K_2O/BaO ratio on crystallization, microstructure and dielectric properties of strontium titanate borosilicate glass ceramics. *Ceram Int* 2004;**30**:477–83.

[18]. Sahu AK, Kumar D, Parkash O. Lead–strontium titanate glass ceramics: II-dielectric behavior. *J Mater Sci* 2006;**41**:2087–96.

[19]. Mori N, Sugimoto Y, Harada J, Higuchi Y. Dielectric properties of new glass–ceramics for LTCC applied to microwave or millimeter-wave frequencies. *J Eur Ceram Soc* 2006;**26**:1925–8.

[20]. Thakur OP, Kumar D, Parkash O, Pandey L. Dielectric behaviour of strontium titanate glass ceramics with bismuth oxide addition as nucleating agent. *Ind J Phys* 1997;**71A**:161–72.

[21]. Moulson AJ, Herbert JM. *Electroceramics*. 2nd ed. England: Wiley; 2003. p. 71–82.

[22]. Vogel W. *Chemistry of glass*. Columbus, OH: The American Ceramic Society; 1985. p. 119–20.

[23]. Tredway WK, Risbud SH, Bergeron CG. Characterization of metastable phases preceding crystallization of a $PbO–SiO_2–TiO_2–Al_2O_3$ glass. In: Simmons JH, Uhlmann DR, Beal GH, editors. *Advances in ceramics, nucleation and crystallization in glasses*, vol. 4. Columbus, OH: The American Ceramic Society; 1982. p. 163–8.

[24]. Thakur OP, Kumar D, Parkash O, Pandey L. Crystallization, microstructure development and dielectric behaviour of glass ceramics in the system $[SrO^{\bullet}TiO_2]–[2SiO_2{}^{\bullet}B_2O_3]–La_2O_3$. *J Mater Sci* 2002;**37**:2597–606.

[25]. Murali Krishna G, Anila Kumari B, Srinivasa Reddy M, Veeraiah N. Characterization and physical properties of $Li_2O–CaF_2–P_2O_5$ glass ceramics with Cr_2O_3 as a nucleating agent—physical properties. *J Sol State Chem* 2007;**180**:2747–55.

[26]. Moulson AJ, Herbert JM. *Electroceramics*. 2nd ed. England: Wiley; 2003. p. 23–4, 34–41.